Estuaries and Coasts
https://doi.org/10.1007/s12237-018-0463-y

Wave Attenuation by Oyster Reefs in Shallow Coastal Bays

Patricia L. Wiberg[1] · Sara R. Taube[1] · Amy E. Ferguson[1] · Marnie R. Kremer[1] · Matthew A. Reidenbach[1]

Received: 16 August 2017 / Revised: 7 September 2018 / Accepted: 13 September 2018

Abstract

Oyster reef restoration in shallow estuarine environments has been thought to have the potential to provide shoreline protection as well as oyster habitat. This study was designed to address the question of how effective oyster reefs are at attenuating wave energy in shallow coastal bays. Measurements were made of waves on both sides of four restored intertidal oyster reefs and at a control site with no reef; mean water depths ranged from 0.9 to 1.3 m. The reefs differed in composition and position relative to the shoreline, but all had reef crest elevations between 0.3 and 0.5 m below mean sea level. Differences in wave heights between the exposed/sheltered sides and upwind/downwind sides of the reefs were used to quantify the effects of the reefs on waves under varying tidal and wind conditions. All four reefs were able to reduce wave heights by an average of 30–50% for water depths of 0.5–1.0 m (bracketing the heights of reef crests) and 0–20% for water depths of 1.0–1.5 m (reef crests > 0.25 m below the water surface). For water depths greater than 1.5 m, there was < 10% change in wave heights. In contrast, there was no average decrease in wave height from the more seaward (exposed) to the more landward wave gauge at the control site regardless of water depth. Based on our results, we conclude that fringing oyster reefs can reduce the wave energy reaching the shoreline of marshes with edge elevations close to mean sea level. However, reefs like those in our study have little effect on waves during deeper water conditions, which allow for the largest waves, and are therefore less likely to offer protection to marshes characterized by high edge scarps and marsh surface elevations well above mean sea level.

Keywords Oyster reefs · Salt marsh · Wave attenuation · Shoreline stabilization · Shallow coastal bays

Introduction

Oyster reefs are known to stabilize intertidal sediment and to influence hydrodynamic patterns within estuarine environments (Dame and Patten 1981; Meyer et al. 1997; Piazza et al. 2005; Coen et al. 2007; Whitman and Reidenbach 2012). Because of their potential stabilizing effects, building oyster reefs close to eroding intertidal marshes has been considered a means of slowing or reversing shoreline erosion (Meyer et al. 1997; Piazza et al. 2005; Stricklin et al. 2009; Scyphers et al. 2011). Modeling of energy flows through oyster reefs shows that reefs change water current patterns (Dame and Patten 1981) and can increase the coefficient of drag up to five times over that for a bare mud bed (Whitman and Reidenbach 2012).

Marshes fringing coastal bays are undergoing rates of lateral erosion in excess of 1 m year^{-1} in many locations (Wray et al. 1995; Day Jr. et al. 1998; Schwimmer 2001; van der Wal and Pye 2004; Wilson and Allison 2008; Marani et al. 2011; Mariotti and Fagherazzi 2013; McLoughlin et al. 2015). Waves are the primary driver of marsh edge erosion in shallow coastal bays (Möller et al. 1999; Tonelli et al. 2010; Marani et al. 2011; Mariotti and Fagherazzi 2013; McLoughlin et al. 2015; Leonardi et al. 2016). Oyster reefs, like coral reefs (Lowe et al. 2005; Huang et al. 2012), may be effective at dissipating wave energy, and thereby slowing retreat of marshes fronted by oyster reefs.

Several previous studies have investigated the efficacy of oyster reefs as a form of erosion control. Meyer et al. (1997), Piazza et al. (2005), and Stricklin et al. (2009) measured shoreline response to restored oyster reefs constructed of old shell material (cultch) placed into relatively low-lying fringing reefs (heights of 0.15–0.7 m) adjacent to intertidal marshes at sites in North Carolina, Louisiana, and Mississippi, respectively. The results revealed considerable variability among

Communicated by Carl T. Friedrichs

Electronic supplementary material The online version of this article (https://doi.org/10.1007/s12237-018-0463-y) contains supplementary material, which is available to authorized users.

✉ Patricia L. Wiberg
pw3c@virginia.edu

[1] Department of Environmental Sciences, University of Virginia, P.O. Box 400123, Charlottesville, VA 22904-4123, USA

Published online: 25 September 2018

sites and generally indicated that reefs are only successful at limiting erosion in low-energy environments (Piazza et al. 2005; Stricklin et al. 2009). None of these studies measured the effects of the constructed reefs on wave attenuation.

Scyphers et al. (2011) constructed and monitored breakwater reefs of loose shell placed on geotextile fabric and shaped into trapezoidal sections 5 m wide, 25 m long with their tops initially just above mean-lower low water (MLLW) at two sites in Alabama. They measured shoreline position, deposition, oyster recruitment, fish, and mobile invertebrates at the constructed reefs and control sites over a 2-year period; no measurements were made of the effect of the reef on waves. The seaward extent of vegetation, which they used to indicate shoreline position, retreated at both sites for both treatments (with and without the breakwater reef), and rates of retreat were not significantly different between treatments. However, Scyphers et al. (2011) did find that the constructed reefs provided habitat for oyster recruitment and were host to larger and more diverse populations of fishes and mobile invertebrates than control sites.

Our study was designed to address the question of how effective oyster reefs are at attenuating wave energy in shallow coastal bays. We considered both established reefs that were located near marshes and newly constructed fringing reefs made using concrete "oyster castle" spat blocks (Theuerkauf et al. 2015). These reefs, which are relatively long, narrow, and offset from the marsh shoreline, are typical of many of the constructed reefs in the Virginia coastal bays. We measured waves and tides on both sides of four study reefs and a control site and used differences in wave heights across the reefs to investigate the impact of reefs on waves under varying tidal and wind conditions.

Study Area

The reefs investigated in this study were located in northern Ramshorn Bay and in northern South Bay, both shallow bays on the seaward side of the southern Delmarva Peninsula in Virginia, USA (Fig. 1). Ramshorn Bay is about 10 km long and 1–2 km wide, with its long axis generally aligned with the long axis of the Delmarva Peninsula (north-northeast (NNE) to south-southwest (SSW)) (Fig. 1a). The bay has a mean depth of 1.1 m relative to mean sea level (MSL) and is fringed with salt marsh around most of the bay. A deeper channel runs through the bay that connects to a larger channel to the south that extends to the Sand Shoal tidal inlet. Although the northeastern end of Ramshorn Bay is open to an adjacent bay (Outlet Bay), circulation in Ramshorn Bay is relatively restricted, resulting in water residence times ranging from 3 to 12 days for the northern-southern portions of the bay, respectively (Safak et al. 2015). South Bay, located between Wreck Island and Mockhorn Island, is 4–5 km wide and 11 km long, with a mean depth of 0.8 m relative to MSL (Fig. 1b). South Bay is relatively well flushed (residence times of < 1 to 4 days; Safak et al. 2015) owing to tidal exchange through Sand Shoal Inlet to the north and New Inlet in the southern portion of the bay.

Mean tidal range in the bays is 1.2–1.3 m (Fig. 2a). Winds in the vicinity of the Virginia coastal bays blow predominantly along the axis of the Delmarva Peninsula with the highest winds from the NNE and the most frequent winds from the SSW (Fig. 2b). When winds blow from the NE, water depths tend to be higher than average (Fig. 2c; Fagherazzi et al. 2010). SW winds are associated with lower than average water levels.

Two oyster reefs were built near small marsh islands adjacent to the Boxtree farm region of northern Ramshorn Bay in the 1950s or 1960s (Truitt, personal communication). The oysters that settled on these reefs were American eastern oysters, *Crassostrea virginica*. The base of the Boxtree southern reef (site BTS) was made of crushed whelk shells, while the Boxtree northern reef (site BTN) was constructed of concrete oyster castles on the shoreward end and old oyster shells on the seaward end (Fig. 3a, b). The BTN reef is nearly perpendicular to the mainland; the BTS reef is about 30° clockwise from perpendicular (Fig. 1a). A third reef, BTI ("Idaho Reef"), was constructed in the same region of interlocking oyster castle spat blocks by The Nature Conservancy (TNC) in 2013 and 2014 (Fig. 3c) on top of an older, dead oyster reef to test the efficacy of oyster castle reefs for mitigating marsh edge erosion and providing substrate for oyster recruitment. This reef is located outside an embayment and roughly parallels the shoreline of the bay interior, which is located about 0.5 km west-northwest of the reef (Fig. 1a). We selected a control site (no reef; site BTC) just south of the Idaho Reef to compare wave conditions at sites with and without reefs. The fourth reef was built by TNC in 2017 at the southern end of the northeast facing side of Man and Boy marsh (site MBE; Fig. 1b) to investigate its effectiveness for wave attenuation and shoreline stabilization. The main reef, made of staggered rows of interlocking oyster castle spat blocks placed on top of a layer of fossil oyster and whelk shell (Fig. 3d), is 26 m away from, and roughly parallels an ENE-facing section of marsh shoreline (Fig. 1b). There is a set of older, degraded oyster spat blocks several meters bayward of the 2017 reef (Fig. 3d).

The estimated fetch for the Boxtree sites is < 1–6 km, with the largest fetch to the southwest and moderate fetch to the east. The sites had very limited fetch to the west and north (Fig. 1a). Woodhouse Jr. and Knutson (1982) considered low-energy environments to have fetch distances of less than 9 km in their study of successful marsh restoration along the Atlantic and Gulf coasts, which was comparable with the fetch range at the Boxtree sites. The limited fetch in this area is reflected in low values of wave exposure and shoreline change. Values of relative wave exposure (RWE; Malhotra and Fonseca 2007) are less than 100 J/m along the continuous shoreline to the west and north of the study sites compared

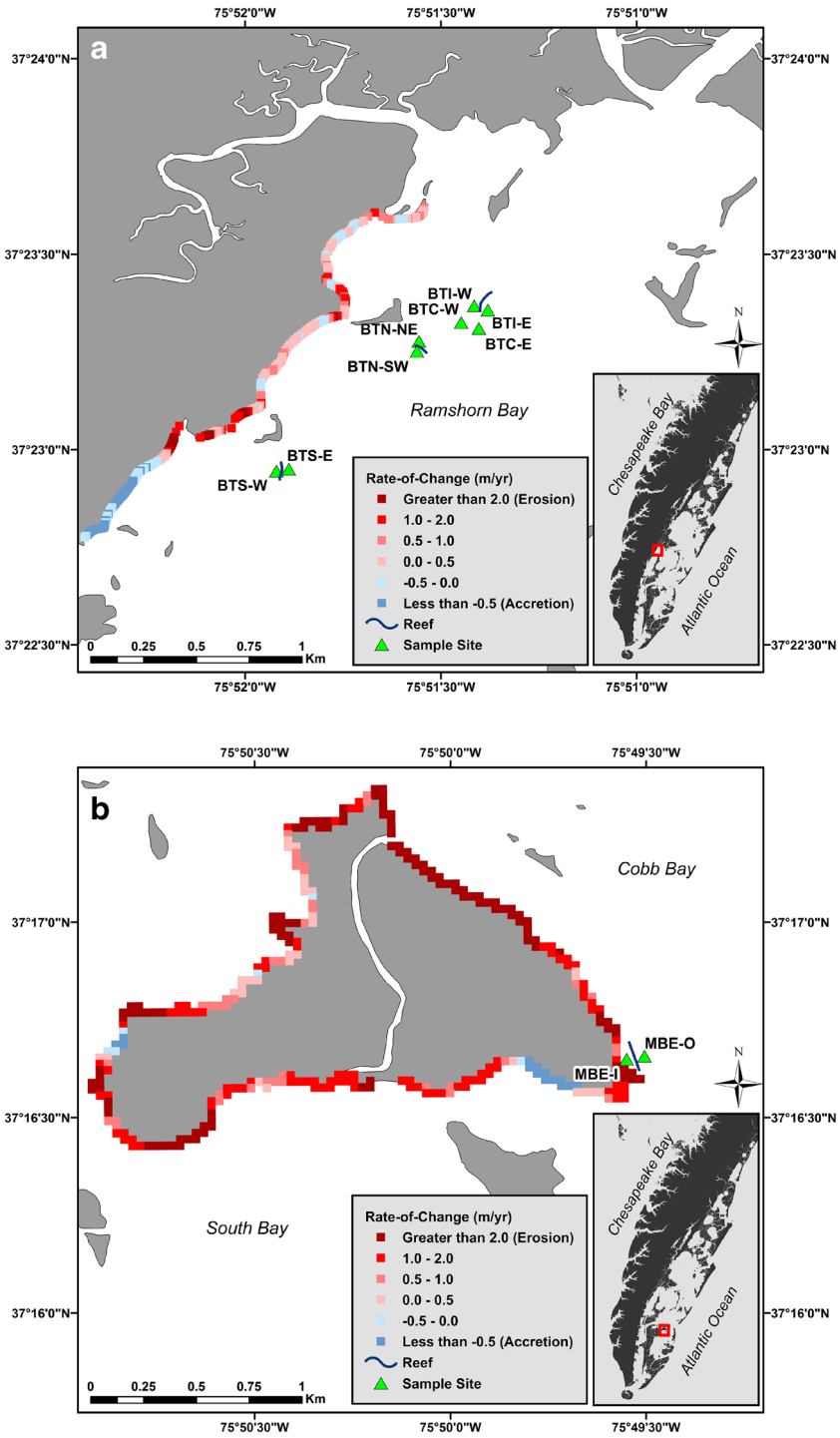

Fig. 1 **a** Study area map showing the shoreline of the northern (Boxtree) region of Ramshorn Bay, VA, with reef crest and wave gauge locations indicated for the BTS, BTN, and BTI reefs and the control site (BTC). **b** Study area map showing the shoreline of the Man and Boy marsh, with reef crest and wave gauge locations indicated for the MBE reef. Colored squares indicate rates of shoreline change from 2006 to 2014 with blues and pinks indicative of accretion and erosion, respectively, as indicated in the legend. Insets show study areas in relation to the lower Delmarva Peninsula and Chesapeake Bay

with values almost ten times higher on the northeast facing side of Man and Boy marsh (Ferguson 2018), where estimated fetch is 2–20 km. The longest fetch at our Man and Boy marsh site is to the NNE, which is also the direction from which the strongest winds blow.

Rates of shoreline change (colored cells along shoreline in Fig. 1) were estimated using the AMBUR method (Jackson et al. 2012) with shorelines digitized from georectified imagery for 2006, 2009, and 2014 available from the National Agricultural Imagery Program (NAIP; gdg.sc.egov.usda.gov) (Emery 2015; Ferguson 2018). Shoreline change in the Boxtree region averaged −0.2 m year^{-1} (erosion), with a standard deviation of 0.7 m, except for the channel mouth area to the west of BTS where rates of erosion were locally higher (Fig. 1a). Rates of shoreline change are larger on Man and Boy marsh, with rates

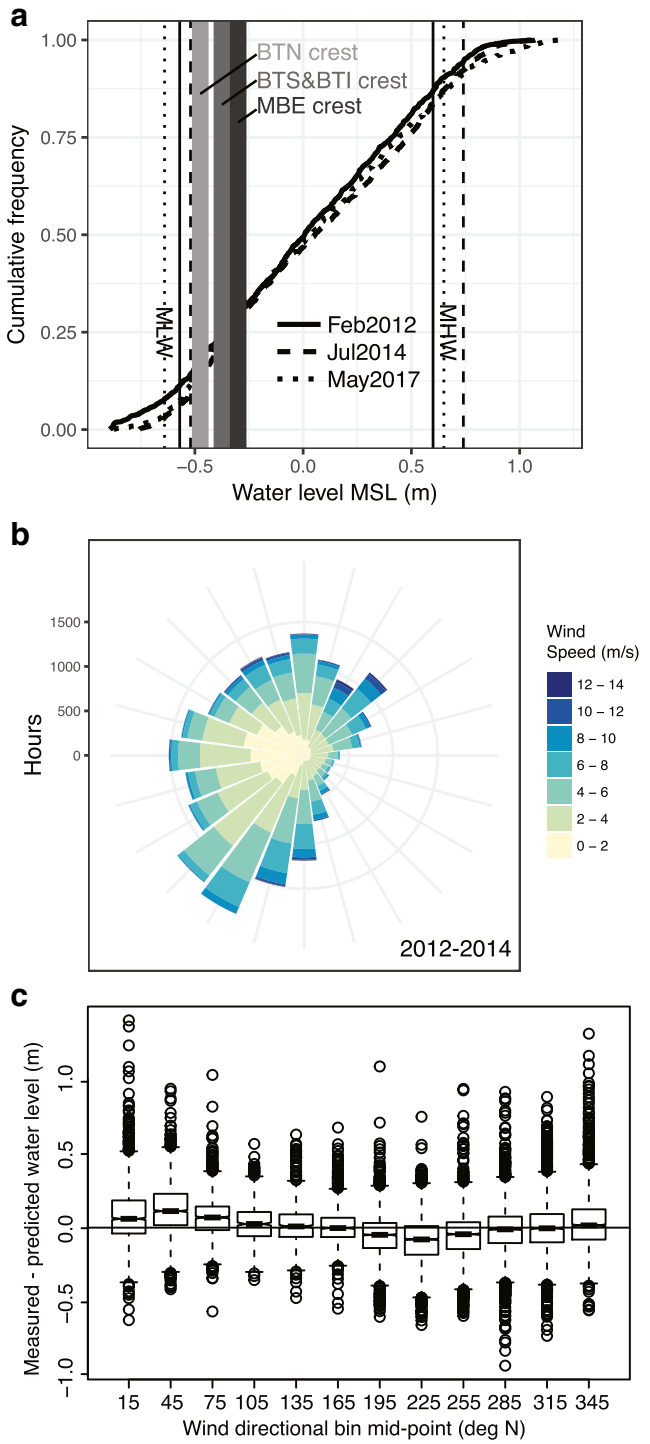

Fig. 2 **a** Cumulative distribution of water levels relative to mean sea level (MSL) during the February 2012, July 2014, and May2017 deployments. Mean low water (MLW) and mean high water (MHW) are indicated for each deployment as is the depth of the reef crests below MSL. **b** Distribution of wind speed and direction for the period January 2012–December 2014 based on measurements at the NOAA station in Wachapreague (station 8631044), corrected to produce best agreement with nearby, but incomplete, wind measurements at Fowling Point (Supplement A, Fig. 1). **c** Distribution of the difference in measured and predicted water levels at Wachapreague for 2012–2014 as a function of wind direction

Fig. 3 Photographs of the study reefs at Boxtree South (BTS, crushed shell), Boxtree North (BTN, oyster shell and oyster castles), Idaho Reef (BTI, oyster castles), and southeastern Man and Boy marsh (MBE). The photograph of BTI was taken shortly after reef construction. The blocks comprising the reef are now covered with oysters

exceeding -1.0 m year^{-1} (erosion) along most of the NE facing side of the island (Fig. 1b), including the site of the constructed reef (MBE).

Methods

Field Measurements

We measured waves and tides on both sides of each study reef and the control site using RBR-Global tide and wave recorders (TWR-2050P; referred to here as a wave gauges), which were placed a distance of roughly 10 m away from both sides of each reef; wave gauges were ~20 m apart at the control site (Fig. 1). At MBE, the wave gauges were placed 10 m on either side of the main (2017) reef; remnants of an older reef (Fig. 3d) were present between the 2017 reef and the bayward wave gauge. The wave gauges recorded tidal elevation and wave conditions every 30 min for 3–4 weeks (Table 1), with tides averaged over a 10-min sampling interval and waves recorded at 4 Hz for 5 min. Nortek AquaDopp Profilers (ADP) were deployed just behind the landward tip of reefs BTS and BTN to characterize current velocities. Velocity was recorded every 30 min for 2 weeks (Table 1), averaging over an interval of 10 min at 0.5 m increments of elevation within the water column, the minimum for the ADP used in this study, with a blanking distance of 0.2 m above the bottom. Velocities reported herein are from the lowest measurement bin.

Table 1 Hydrodynamic sampling sites and schedule

Site/instrument[a]	Start date	End date	Lat N	Lon W	Average depth (m)
BTS					
ADP	7 Jul 2011	21 Jul 2011			
RBR-W	15 Feb 2012	7 Mar 2012	37 22.945	75 51.920	1.15
RBR-E	15 Feb 2012	7 Mar 2012	37 22.950	75 51.888	1.11
BTN					
RBR-NE	15 Feb 2012	7 Mar 2012	37 23.251	75 51.561	1.15
RBR-SW	15 Feb 2012	7 Mar 2012	37 23.277	75 51.555	1.24
BTI					
RBR-W	27 Jun 2014	30 Jul 2014	37 23.368	75 51.415	1.22
RBR-E	27 Jun 2014	30 Jul 2014	37 23.357	75 51.380	1.27
BTC					
RBR-W	27 Jun 2014	30 Jul 2014	37 23.325	75 51.448	1.35
RBR-E	27 Jun 2014	30 Jul 2014	37 23.310	75 51.403	1.27
MBE					
RBR-W	9 May 2017	31 May 2017	37 16.625	75 49.575	0.87
RBR-E	9 May 2017	31 May 2017	37 16.626	75 49.589	1.30

Locations are shown in Fig. 1

[a] The east (E) sides of BTS, BTI, and MBE are the more exposed sides of the reefs; exposed side of BTN depends on wave direction (see text)

Tidal and meteorological data for the duration of each deployment were obtained from the NOAA station at Wachapreague, VA, located 30 km north of Ramshorn Bay (tidesandcurrents.noaa.gov; station 8631044). Wind speed and direction were also available from an anemometer positioned 7.5 m above a marsh surface on Fowling Point, about 3.5 km north of the study area, for the BTI/BTC deployment (Kathilankal et al. 2008). Atmospheric pressure recorded at Wachapreague was used to correct pressure measured by the ADP and wave gauges for atmospheric pressure (Wunsch and Stammer 1997), after which the corrected pressure values were converted to water depth. Tidal water levels from the wave gauges, ADP and Wachapreague tide gauge were checked for agreement, as were winds from Wachapreague and Fowling Point (see below).

Elevations of the BTS and BTN reef crests as well as a number of reef cross-sections were surveyed in 2012 using a Trimble RTK system (Taube 2013). The vegetation lines of the adjacent marshes were also surveyed. Elevations were checked against photos of the reef crest at known tidal water elevations. Elevations of the BTI reef were estimated from measurements of water depth to the reef crest at known tidal elevations; similar measurements were made at BTS and BTN to check for consistency. The height of the MBE reef was determined from the spat block assembly and was checked against photos of the reef crest at known tidal water elevations.

Wind Conditions

Wind speeds measured at the Wachapreague NOAA station are consistently lower than winds measured at other met stations in or near the VCR likely due to the elevation of the anemometer and its location on top of a shed (McLoughlin et al. 2015); wind directions measured at sites within the VCR are generally in good agreement. Comparison of wind measurements from Wachapreague and Fowling Point in July 2014 reveals that the largest differences in wind speed were for winds from the northwest (NW; Supplement, Figs. S1 and S2). Winds from both sites were decomposed into NW-SE and NE-SW components. Scatter plots for positive and negative values along each coordinate axis were used to develop wind speed corrections to bring Wachapreague wind into better agreement with the closer and less obstructed record from Fowling Point (Supplement). The same correction was applied to Wachapreague winds in June 2016 and compared with concurrently measured Fowling Point winds as a test of the correction (Supplement, Fig. S3). The corrections were then applied to Wachapreague winds during the February 2012 and May 2017 deployments (no Fowling Point winds at these times) and for the 3-year period from 2012 to 2014 shown in Fig. 2b.

Wave Analysis

Significant wave height for each wave record was obtained using the RBR wave analysis software (Ruskin) based on the variance of the 4-Hz depth-corrected water-surface elevation time series recorded at each site (see, e.g., Wiberg and Sherwood 2008). Changes in wave height across each reef were analyzed based on wind speed, wind direction, total water depth, and water depth above the reef in order to determine

conditions contributing to the greatest wave heights and wave height differences at each site. Comparisons were made of waves on the more exposed side (east sides of BTS, BTI and MBE; southwest side of BTN) vs. more sheltered side of each reef. Comparisons were also made of waves on the upwind vs. downwind sides of each reef, with upwind and downwind sides determined for each record based on wind direction and reef orientation. The upwind/downwind and exposed/sheltered gauge designations at BTC (site with no reef) were set to match those at BTI. Because our wave gauges did not resolve wave direction and our measurements were limited to a single pair of wave gauges per reef, we did not attempt to quantify wave dissipation per se. However, spectra were calculated for a subset of the 5-min-long, 4-Hz records depth-corrected water-surface elevation time series measured by the wave gauges following Wiberg and Sherwood (2008) and examined for differences across the reefs.

Results

Site Characterization

Average water depth at each site is listed in Table 1. The BTS reef averaged 0.7 m high (crest height 0.35–0.4 m below MSL). The main reef structure was 3–5 m wide with gently sloping sides that gradually descend into the mud at the edge of the reef (Taube 2013; Fig. 3a). The shoreward portion of the BTN reef was similar in height to BTS (crest 0.45–0.50 m below MSL owing to slightly deeper water depths at BTN compared with BTS); the width of the main reef structure was 0.5–2 m. This reef comprised two sections, the shoreward section made of oyster castles that had a relatively uniform elevation (Fig. 3b), and an older, lower section made of shell. The difference in surveyed reef-crest elevations below MSL at BTS and BTN (about 0.1 m) is consistent with aerial photos that indicate greater emergence of the BTS reef compared with the BTN reef at low tidal conditions. BTI was 4–5 m wide and uniform in elevation when constructed (Fig. 3c). Reef-top elevation relative to MSL at BTI was similar to BTS (roughly 0.35 m below MSL), but about 0.1 m deeper relative to mean water depth during the deployment owing to seasonal variations in mean water level in the VCR. The MBE reef comprises a 150-m long, 2.6-m wide, 0.5-m high staggered array of spat blocks on top of a layer of shell just inshore of an older similar array of shell and concrete rubble (Fig. 3d). Reef crest elevation is somewhat variable along the reef but was roughly 0.3 m below MSL at the study site.

Mean tidal ranges recorded at the study sites by the wave gauges were 1.26–1.31 m, with reef crests submerged about three quarters of the time (Table 2; Fig. 2a). Current speeds averaged 0.12–0.13 m s^{-1} at BTS and BTN (Table 2). The dominant flow axis was NE/SW, which paralleled the general orientation of the shoreline in the Boxtree study area (Fig. 1a). Water levels measured at NOAA's Wachapreague tide station were very well correlated with water level measurements in the study areas.

During the February 2012 deployment (15 Feb 2012–7 Mar 2012), winds tended to most frequently blow from the southwest, but the highest wind speeds were from the northeast (Fig. 4a). The distribution of winds during this period was similar to the distribution over the 3 years from 2012 to 14 (Fig. 2b). Winds blew predominantly from the southwest during the July 2014 deployment (28 Jun 2014–31 Jul 2014) with less-frequent winds from the east-northeast (Fig. 4b). The southerly winds during the July 2014 deployment were larger on average than the southerly winds during the February 2012, whereas winds from the north-northeast were more frequent and larger during the February 2012 deployment than the July 2014 deployment. Several periods of strong northeasterly winds marked the May 2017 deployment, with remaining winds primarily from the south-southwest (Fig. 4c). Winds ≥ 8 m s^{-1} were most frequent in May 2017 (15% of the record) but accounted for < 1% of all wind speeds in February 2012 and July 2014.

Wave Environment

Average significant wave heights of 0.03, 0.06–0.07, and 0.10 m were recorded in February 2012, July 2014, and May 2017, respectively (Table 2). Maximum significant wave heights were 0.3–0.4 m during the Boxtree deployments and reached 0.5 m at MBE. Cumulative distributions of wave heights indicate that waves at BTS-E (more exposed side) were consistently higher than at BTS-W and both wave gauges at BTN, all of which had roughly the same distribution (Fig. 5a). Overall, the waves at BTI were a little larger than at BTC (Fig. 5b), and the largest waves recorded at BTC were at the more western (shoreward) site (BTC-W). Wave heights on the more seaward and deeper side of the reef at MBE (MBE-E) were consistently a little higher than on the marshward side (MBE-W; Fig. 5c). Wave period at all sites was roughly 2 s.

Of more importance for the present study than wave height per se is the difference in wave heights across the reefs. Statistics of least-square linear relationships (Table 3) between waves measured simultaneously on both sides of the reefs (gauges 20 m apart) show a reduction in wave height from the more bayward/exposed side (east sides of BTS and MBE; southwest side of BTN) to the more landward, sheltered side of BTS, BTN, and MBE. These fits indicated no significant difference on average from the east side to the west side of BTI and an increase in wave height from the eastern (bayward) to the western (landward) gauge at BTC (site with no reef).

While it was relatively straightforward to identify the more exposed and more sheltered sides of the BTS, BTI, and MBE

Table 2 Summary of measurements at the sampling sites

	BTS	BTN	BTI	BTC	MBE17
Tides (m MSL)					
Mean (max) high	0.60 (1.06)	0.60 (1.06)	0.74 (1.08)	0.74 (1.08)	0.65 (1.13)
Mean (min) low	− 0.57 (− 0.97)	− 0.57 (− 1.02)	− 0.52 (− 0.73)	− 0.52 (− 0.75)	− 0.64 (− 0.94)
Fraction of time reef crest exposed	0.26	0.19	0.22	N/A	0.35
Average current speed[a] (m s^{-1})	0.13	0.12			
Dominant current direction	ENE, WSW	ENE, W			
Significant wave height (m; mean/max)	0.03/0.38	0.03/0.33	0.07/0.32	0.06/0.43	0.10/0.52
Fraction of time E/NE side of reef is upwind	0.27	0.30	0.34	0.34	0.51

[a] Velocity measured at BTS and BTN only

reefs, drawing this distinction was more difficult at the BTN reef because of its orientation perpendicular to the adjacent marsh. Although the northern side of BTN faced into a more sheltered portion of the bay (Fig. 1a), winds from the northeast could generate waves that approached the reef from its northern side, particularly under high water conditions when the marshes to the northeast were submerged. To account for this, statistics of least-square linear relationships (Table 3) were also calculated for waves from the upwind vs. downwind sides of the reefs, defined simply in terms of wind direction relative to the orientation of the reef crest-line. Wave heights were on average consistently lower (slope significantly < 1) on the downwind compared with upwind sides of all four reefs (Table 3); there was no significant difference for the control site BTC.

The largest overall reduction in wave heights, 17–19% as indicated by the slope of the line fit to a scatterplot of significant wave heights on the two sides of a reef, was found at BTS (Fig. 6a; Table 3). The slope was not significantly different when considered in terms of waves on the more exposed (eastern) vs. more sheltered (western) side of BTS or waves on the upwind vs. downwind side of BTS, largely because most of the stronger winds came from the more exposed side of BTS. A smaller overall reduction of 4% was found for the upwind vs. downwind side of the BTN reef (10% for SW vs. NE side; Fig. 6b; Table 3). At BTI, an overall reduction in significant wave height of 7% was found for waves on the upwind vs. downwind side; no difference was observed for waves on exposed (eastern) vs. sheltered side of this reef, which roughly paralleled the shoreline (Fig. 6c). Waves at BTC (no reef control site), increased in height by about 6% toward the shoreline (Fig. 6d), but were unchanged on average on the downwind vs. upwind side (Table 3). At MBE, the slope was not significantly different for wave on the more exposed (eastern) vs. more sheltered side of MBE compared with waves on the upwind vs. downwind side of MBE, with a 13–16% overall reduction in wave height (Table 3). Like BTS, this is because the strongest winds blew from the more exposed side of the reef.

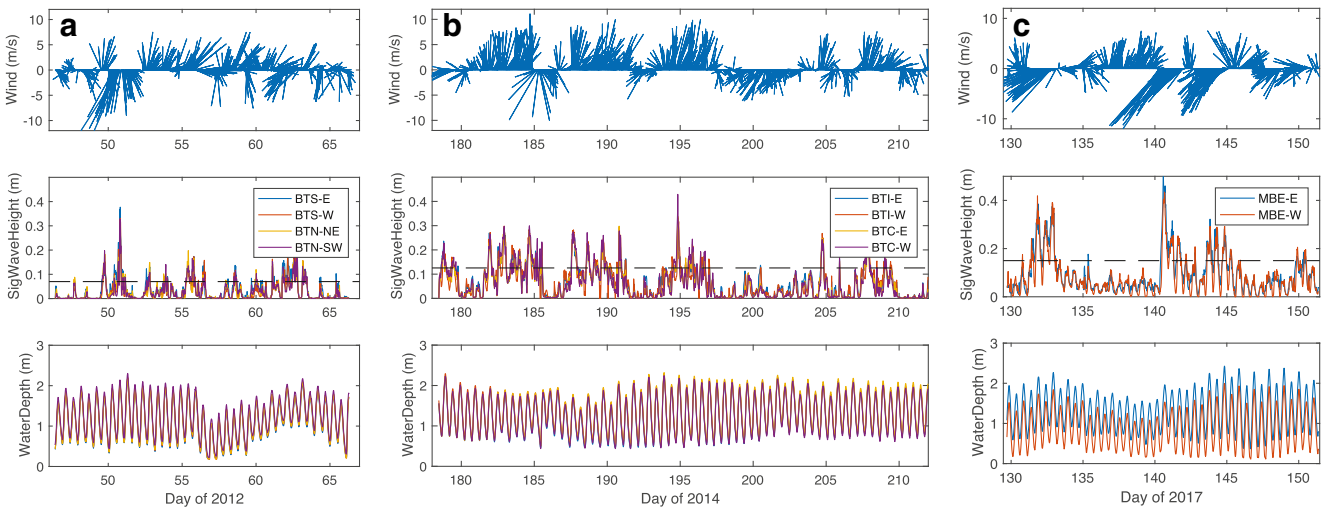

Fig. 4 Wind, wave, and water depth time series for the **a** February 2012, **b** July 2014, and **c** May 2017 deployments. The wind vectors are pointing in the direction the wind is blowing, and the length is proportional to wind speed as indicated in the *y*-axis. The horizontal dashed lines in the middle panels indicate the event threshold for waves during each deployment, defined as one standard deviation above the mean

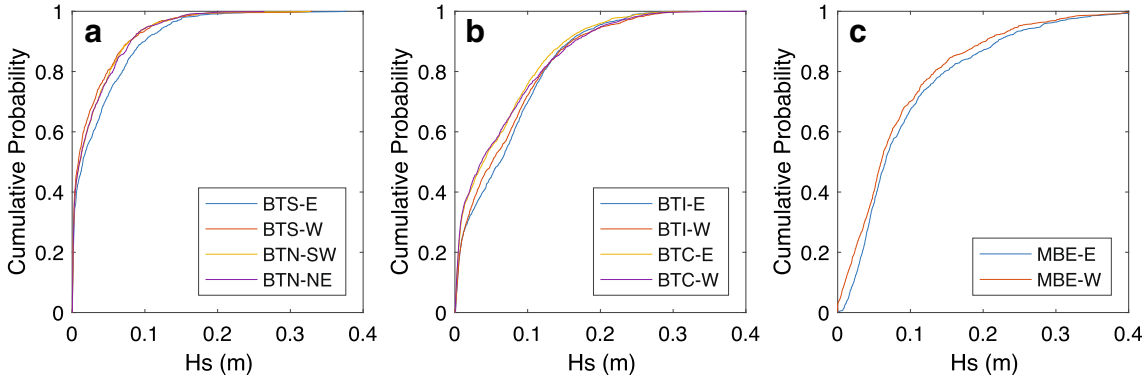

Fig. 5 Cumulative distributions of significant wave height during the **a** February 2012 deployment, **b** July 2014 deployment, and **c** May 2017 deployment

Effects of Water Depth and Wind Speed

Owing to the relatively large changes in wave height that were observed across the BTS reef, this site provides an interesting set of measurements to investigate in more detail. Figure 7a depicts all wave measurements at BTS-E (more exposed side of reef) in terms of wind speed and water depth at the time the waves were recorded. Low wind speeds (< 2.5 m s^{-1}) and shallow water depths (< 0.5 m) consistently are associated with very small waves. Wave heights increase with water depth and wind speed, with the largest waves recorded for northeasterly winds of 9–12 m s^{-1} and water depths of 2 m. Changes in significant wave height across the reef from BTS-E to BTS-W are shown in a similar manner in Fig. 7b. The greatest change in wave height is found for moderate wind speeds and water depths in the range of 0.6–1.1 m. Reef crest height at BTS was 0.7–0.8 m above the bay bottom.

To extend this comparison with the other sites and to provide a more quantitative comparison of change in wave height as a function of water depth, the regression analysis of waves on both sides of the reefs was extended by dividing the data into times when water depths were shallower and deeper than 1.0 m (Fig. 6; Table 3). At all sites, reef crests were submerged by at least 0.25 m of water at a water depth of 1.0 m. For all four reef sites, the change in wave heights across the reef was significantly greater for shallower water depths than deeper conditions (Fig. 6; Table 3), averaging 30–70% reduction in wave height. At BTS and MBE there was also a more modest but significant reduction of wave heights for deeper-water conditions (13–15% compared with 50–70% reduction for shallower depths; Table 3). In

Table 3 Comparison of waves across reefs

	BTS	BTN	BTI	BTC	MBE
Bayward vs. landward side of reef[a]					
Slope (with 95% confidence interval) of least-square line	0.81 (0.02)	0.90 (0.02)	1.0 (0.02)	1.06 (0.01)	0.87 (0.02)
Intercept (with 95% confidence interval) of least-square line	− 0.002 (0.001)	0.003 (0.001)	− 0.002 (0.002)	− 0.002 (0.001)	0.002 (0.003)
R^2	0.87	0.85	0.90	0.97	0.84
Upwind vs. downwind side of reef					
Slope (with 95% confidence interval) of least-square line	0.83 (0.02)	0.96 (0.03)	0.93 (0.01)	1.01 (0.01)	0.84 (0.02)
Intercept (with 95% confidence interval) of least-squares line	0.004 (0.001)	0.000 (0.001)	− 0.001 (0.002)	0.002 (0.001)	0.006 (0.003)
R^2	0.83	0.85	0.90	0.96	0.84
Water depths deeper and shallower than 1.0 m[b]					
Deeper: slope	0.87 (0.02)	1.03 (0.03)	1.04 (0.01)	1.05 (0.01)	0.85 (0.02)
Intercept	− 0.001 (0.001)	0.001 (0.002)	0.001 (0.001)	− 0.001 (0.001)	0.015 (0.003)
R^2	0.95	0.91	0.97	0.97	0.91
Shallower: slope	0.50 (0.04)	0.55 (0.04)	0.69 (0.05)	1.12 (0.02)	0.28 (0.03)
Intercept	0.001 (0.002)	0.002 (0.001)	0.006 (0.004)	− 0.004 (0.002)	0.003 (0.002)
R^2	0.57	0.65	0.58	0.96	0.52

[a] For BTN, which is perpendicular to the shoreline, the regressions were of the SW-facing side (toward more open water) vs. the NE-facing side

[b] Bayward vs. landward sides of BTS, BTI, BTC, and MBE; upwind vs. downwind side of BTN

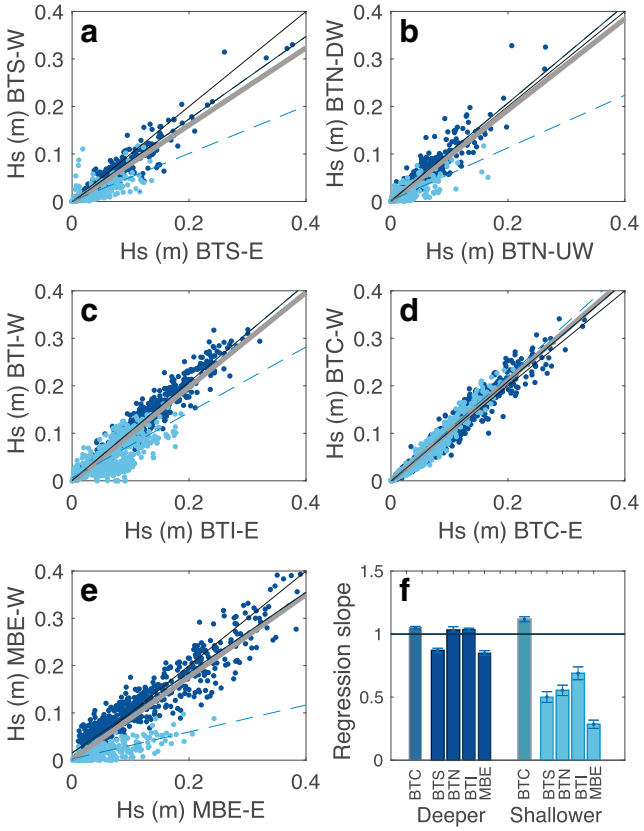

Fig. 6 Scatter plots of significant wave height recorded on the eastern (more exposed) vs. western sides of study reefs **a** BTS, **c** BTI, **d** BTC (the control site with no reef), and **e** MBE. **b** Scatter plot-significant wave height recorded on the upwind vs. downwind sides of study reef BTN. Dot color indicates whether water was ≤ 1.0 m (light blue) or > 1.0 m (dark blue). The solid black line is the 1:1 line, the thicker gray line is the best fit line to all points, the light blue dashed line is the best fit for depths ≤ 1.0 m, and the dark blue dashed line is the best fit for depths > 1.0 m (Table 3). **f** Summary of regression slopes indicated in (**a**)–(**e**) for deeper (> 1.0 m) and shallower (≤ 1.0 m) water depths; the shaded bar to the left of each set is for BTC, the control site with no reef. All wave gauge pairs were 20 m apart

contrast, the control site BTC (no reef) showed a distinctly different pattern of wave height difference for shallow-water conditions, with 12% larger waves on average at the more shoreward (western) of the pair of wave gauges at BTC.

Wave spectra for a subset of cases from the Boxtree site with moderately high winds from NE and SW and water depths in the shallower (< 0.75 m), intermediate (0.75–1.0 m), and deeper (> 1.0) range (Fig. 8) further illustrate the effects of water depth on wave conditions across the reefs. In each row of Fig. 8, spectra are shown for the same times at sites BTS and BTN (in February 2012) and at sites BTI and BTC (in July 2014). Times, winds, water depths and significant wave heights for each case are given in Table 4. For these reefs, depth was similar on both sides of the reef, allowing differences in spectra across the reef to be largely attributed to the reef itself. Spectra for site MBE were not included in Fig. 8 owing to significant differences in depth between the two wave gauges at that site that make it difficult to separate spectral differences caused by change in water depth from differences due to the presence of the reef.

Wave Events

Because wave energy is proportional to wave height squared, the smallest waves, which are also the most frequent waves, have little effect on the bay bottom or adjacent marshes. We used an event threshold of one standard deviation above mean significant wave height for all wave gauges during each deployment. This yielded an event threshold of 0.07 m for February 2012, 0.13 m for July 2014, and 0.17 m for May 2017. After removing wave records with significant wave heights below the event threshold, 12–16% of the half-hourly wave records remained for the five sites. Wind directions during these events were primarily from the northeast and south-southwest, consistent with the directions typically associated with the highest winds in the study area (Fig. 2b). The strong tidal modulation of waves during the intervals of high winds is evident in all records (Fig. 4), such that the largest percentage of wave conditions exceeding the threshold occurred when water depths were relatively high.

While the largest waves were recorded when water depths and wind speeds were both large, the largest average change in wave heights for waves exceeding the event threshold was observed for shallow - intermediate water depths (Fig. 9; Table 5). Similar to the pattern found for all waves (Fig. 6), waves exceeding the event threshold experienced the greatest average reduction in wave height across the reefs at water depths in the range of 0.5–1.0 m, spanning the heights of the reef crests. Within this depth range, event wave heights at the BTS, BTN and BTI reefs were reduced by an average of 0.05 m, representing 30–50% of the incoming wave height (Table 5). Average wave height reduction was larger at MBE, where waves were also larger, averaging 0.10 m, but the fractional change (47%) of the incoming wave height was similar to that at BTS (Table 5). Event wave height differences were significantly smaller at all four reef sites for water depths greater than 1.0 m (0.0–0.3 m below MSL at the reef locations), averaging 0–20% for depths of 1.0–1.5 m and < 10% for depths > 1.5 m (Table 5; Fig. 9). This stands in contrast with observed wave differences at the control site (BTC) where event wave heights were consistently larger at the more landward of the pair of wave gauges.

Discussion

Our results show that oyster reefs can significantly reduce wave heights, and therefore wave energy, within a range of intermediate water depths from several tens of centimeters below a reef crest to several tens of centimeters above the crest. At lower

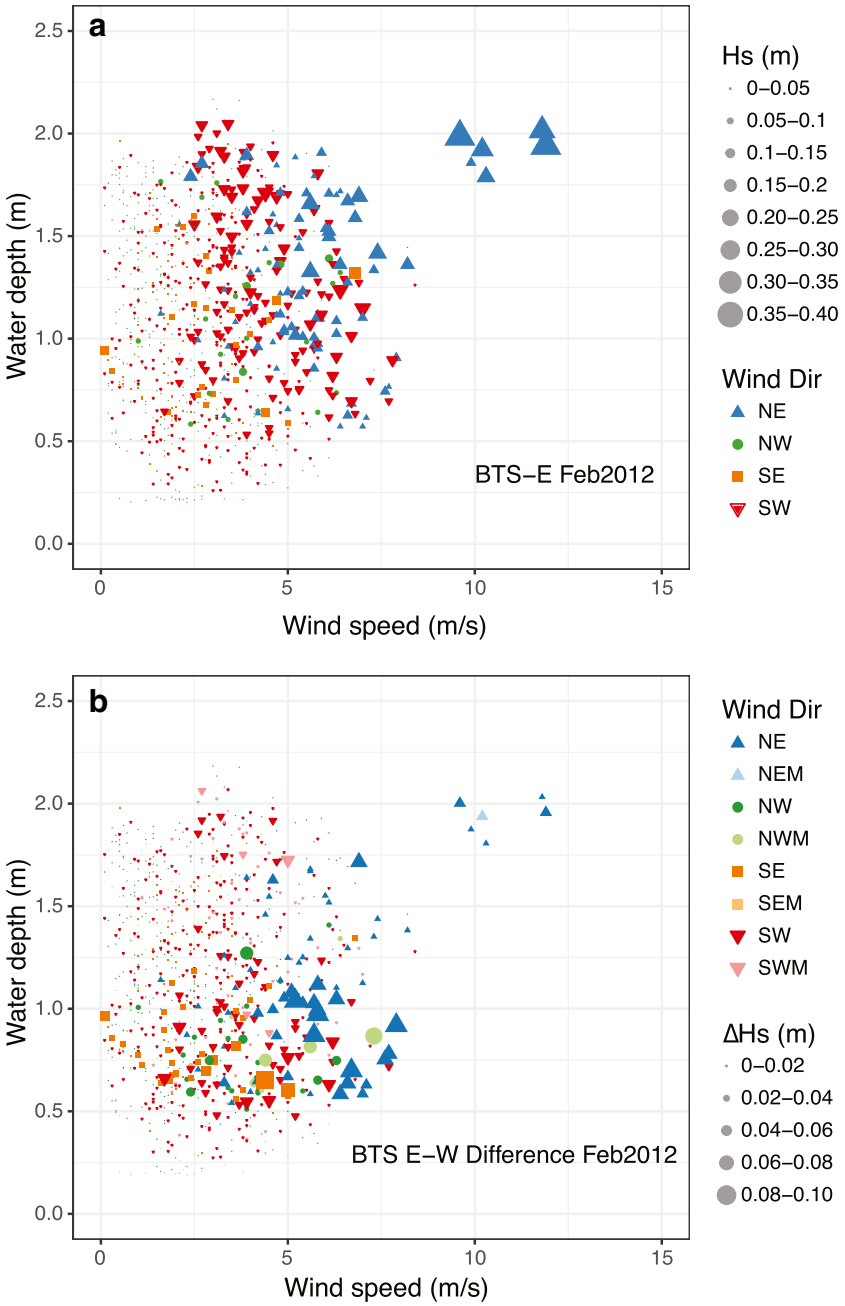

Fig. 7 **a** Significant wave height (as indicated by symbol size; see legend) as a function of wind speed and water depth for the BTS-E wave gauge (Fig. 1a). Wind direction (0–90 = NW, 90–180 = SE; 180–270 = SW; 270–360 = NW) is indicate by symbol type and color (see legend). **b** Difference in significant wave height from the eastern (more exposed) to western (more sheltered) sides of BTS. Symbol size indicates the magnitude of the wave height difference and symbol type and color indicate wind direction. For each range of wind directions, e.g., NE (0–90°), the darker shade of each color is indicative of a positive difference in wave height (larger on the eastern side of the BTS reef) while the ligher shade indicates a negative difference in wave height (waves larger on the western side of BTS)

water depths, waves are small regardless of wind speed and are completely interrupted by the emergent reef. At higher water depths, the reefs in our study area had significantly less impact on wave heights. The effects of reef orientation, water depth, and storms on reef-related reductions in wave height are considered below, as well as the potential significance of the observed wave height reductions on nearby marshes.

Reef Orientation Relative to the Shoreline

Our study reefs exhibited a range of orientations with respect to the trend of the shoreline. Reef MBE was parallel to and closest to the shoreline of the four reefs, with the largest fetch and the highest winds on its eastern side (MBE-E; Fig. 1b). Of the five study sites, MBE had the largest difference in depth, 0.4 m, between the pair of wave gauges on either side of the reef, which may contribute to the reduction in wave height recorded between the two wave gauges. This site experienced the highest winds, with all winds ≥ 10 m s^{-1} coming from the offshore direction. As noted above, the highest waves were generally associated with the deepest water, thereby diminishing the potential for the reef to significantly reduce wave heights. However, it is worth pointing out that the three high outliers in the deepest depth range in Fig. 9e are for the

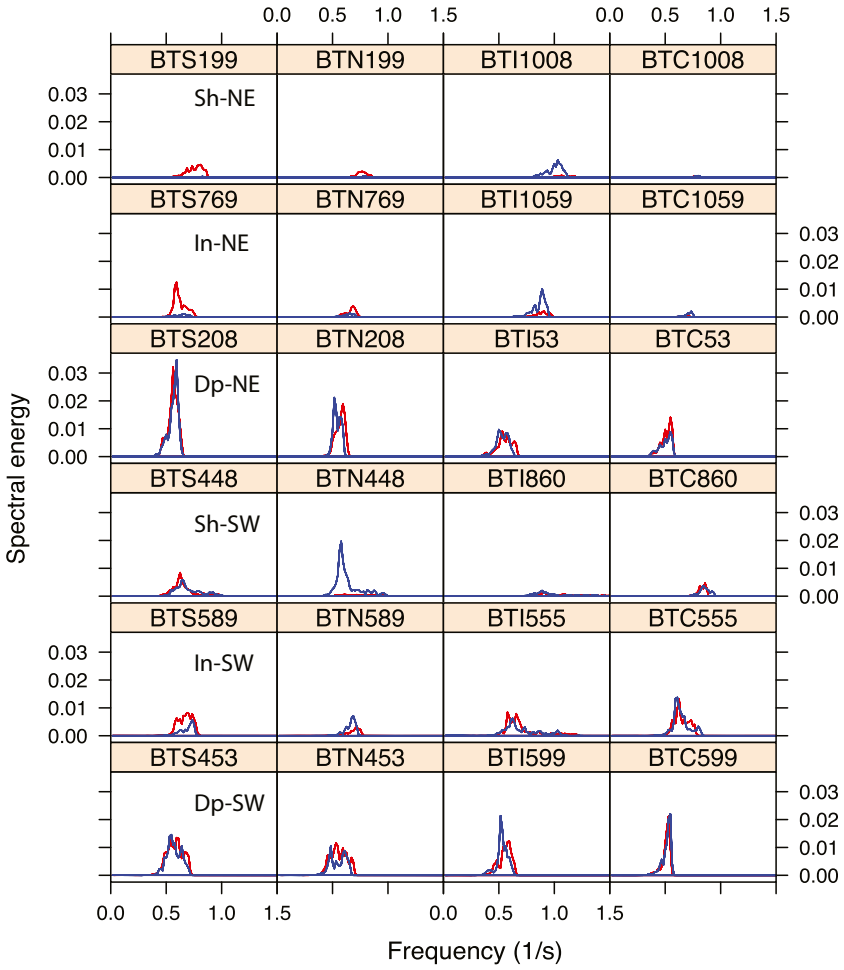

Fig. 8 Wave spectra examples from sites BTS, BTN, BTI, and BTC, by column. The top 3 rows show cases of shallow-, intermediate-, and deep-water conditions for times when winds were blowing from the NE. The lower three rows are for shallow-, intermediate-, and deep-water conditions for times when winds were blowing from the SW. In each case a pair of spectra are shown, with the red curve corresponding to the gauge on the more eastern/north-eastern wave gage and the blue curve corresponding to the western/southwestern side. All pairs of wave gauges were 20 m apart

large northeasterly wind event on yearday 140 (12 May 2017; Fig. 4c) and represent a wave height reduction of 25%. Without more detailed data (directional wave gauges and more sampling locations), it is not possible to say whether these reductions in wave heights under deeper-water conditions are the result of the reef or the decrease in depth between the two wave gauges or some combination of both.

Reef BTI roughly paralleled the general trend of the shoreline, such that the eastern side (BTI-E) was clearly the side with larger fetch and therefore more likely to be impacted by large wind-waves than its western side (Fig. 1a). Any effect of the reef at this site, however, was superimposed on a tendency for waves measured at the same time to increase in height between the outer (BTC-E) and inner (BTC-W) wave gauges at a nearby site with no reef (Fig. 6d; Table 3). Water depths at BTC-E and BTC-W differ by < 10%, making it more likely that the increase in wave height is due to refraction related to the local configuration of reefs and coastal features (Fig. 1a) than shoaling. It does show, however, that BTI is a more effective wave attenuator than indicated by the simple difference in wave height across the reef, because in the absence of the reef, waves at BTI-W would likely have been greater in height than those at BTI-E.

The BTS reef was sub-parallel to the shoreline, but its eastern side (BTS-E) was exposed to a much larger fetch than its western side (Fig. 1a). Cumulative distributions of significant wave heights at this site (Fig. 5a) confirm that waves on the eastern side of the reef were consistently larger than those on the western side. Only one wind event from the west reversed this trend (Fig. 7b, NWM), but these are uncommon (Fig. 2b). During this event, when water depths were below 0.8 m, there were moderate sized waves on the western side of BTS (0.05–0.11 m) but almost no waves on the eastern side (0.01–0.02 m) suggesting the reef crest was emergent. This creates a relatively large negative mean change in wave height (0.44 m smaller on the more exposed, eastern side of BTS) for this event (Figs. 6 and 7). Waves produced by southwest winds have the largest fetch, propagating up the main axis of Ramshorn Bay, seaward of the BTS reef. As a result, waves from the southwest were generally larger on the eastern side of the reef (Fig. 7b). The BTS and BTI reef crests are oriented in a direction similar to that of the dominant winds in the VCR (NNE-SSW). Particularly for winds from the SSW, which allows for greater fetch to the study reefs, waves may at times be reaching both sides of these reefs without crossing their crests.

Table 4 Data corresponding to wave spectra shown in Fig. 8

Date	Time	YrDay	RecNo	WSpd	WDir	Depth	Hs-out	Hs-in	ΔHs
Site BTS, 2012, reef crest orientation ~ 10° east of north									
2/19	1200	50.500	199	11.0	23	0.78	0.100	0.021	0.08
3/2	0900	62.375	769	6.2	59	0.97	0.123	0.043	0.08
2/19	1630	50.688	208	8.4	13	1.34	0.23	0.20	0.03
2/24	1630	55.688	448	8.1	217	0.72	0.122	0.115	0.01
2/27	1500	58.625	589	7.3	233	0.84	0.133	0.085	0.05
2/24	1900	55.792	453	7.6	235	1.25	0.174	0.173	0.001
Site BTN, 2012, reef crest orientation ~ 35° east of north									
2/19	1200	50.500	199	11.0	23	0.82	0.060	0.020	0.04
3/2	0900	62.375	769	6.2	59	1.04	0.072	0.052	0.02
2/19	1630	50.688	208	8.4	13	1.42	0.171	0.153	0.02
2/24	1630	55.688	448	8.1	217	0.82	0.051	0.166	− 0.12
2/27	1500	58.625	589	7.3	233	1.00	0.074	0.096	− 0.03
2/24	1900	55.792	453	7.6	235	1.21	0.167	0.132	0.015
Site BTI, 2014, reef crest orientation ~ 10° east of north									
7/18	1000	199.415	1008	6.1	61	0.70	0.107	0.037	0.070
7/19	1130	200.465	1059	6.7	53	0.98	0.125	0.120	0.005
6/28	1230	179.521	53	5.3	77	1.45	0.128	0.133	− 0.005
7/15	0800	196.323	860	7.0	203	0.75	0.080	0.074	0.006
7/8	2330	189.965	555	7.0	218	0.76	0.119	0.121	− 0.003
7/9	2130	190.883	599	7.0	204	1.47	0.220	0.260	− 0.040
Site BTC, 2014, no reef									
7/18	1000	199.415	1008	6.1	61	0.73	0.027	0.021	0.006
7/19	1130	200.465	1059	6.7	53	1.01	0.061	0.049	0.012
6/28	1230	179.523	53	5.3	77	1.41	0.118	0.133	− 0.015
7/15	0800	196.323	860	7.0	203	0.77	0.091	0.087	0.004
7/8	2330	189.965	555	7.0	218	0.78	0.148	0.149	− 0.001
7/9	2130	190.883	599	7.0	204	1.50	0.258	0.259	− 0.001

The BTN reef, oriented perpendicular to the shoreline trend, was the only one of the four reefs to lack a clear "exposed" vs. "sheltered" side. While a reef with this orientation is unlikely to be built for shoreline protection, it is worth considering the effect that reefs like this (natural or constructed for purposes other than shoreline protection such as provision of oyster habitat) might have on passing waves. Because both sides of the reef were at times exposed to large waves, we found it most useful to think of this reef in terms of its upwind and downwind sides, which varied according to wind direction. This distinction was less useful for the other reefs, because when winds blew from their more sheltered sides (west and northwest), the fetch was generally small enough that the resulting waves were small as well.

The northeastern side of the BTN reef faces into the northern end of Ramshorn Bay (Fig. 1a). There is limited fetch in this direction when water depths are below the elevation of the marshes, but the strongest winds come from the northeast (Fig. 2b). In addition, northeasterly winds tend to be associated with super-elevation of the water surface (storm surge) in the Virginia coastal bays (Fig. 2c; Fagherazzi et al. 2010). Significant submergence of marshes to the northeast could locally increase fetch in this direction. Surprisingly, the period of high northeasterly winds during the BTN deployment (19 Feb 2012; yearday 50), was characterized by relatively high waves on the NE side of BTN (0.19–0.26 m) but even higher waves on the SW side of the reef (0.19–0.33 m). As a result, the upwind-downwind wave height difference was negative (Fig. 6b, upwind-side wave heights > 0.2 m). The larger waves on the downwind side of BTN may have been generated in the more open water to the east and propagated into northern Ramshorn Bay.

Importance of Reef Crest Elevation Relative to the Water Surface

The greatest average decreases in wave heights across the reefs were associated with water depths in the range of 0.5–

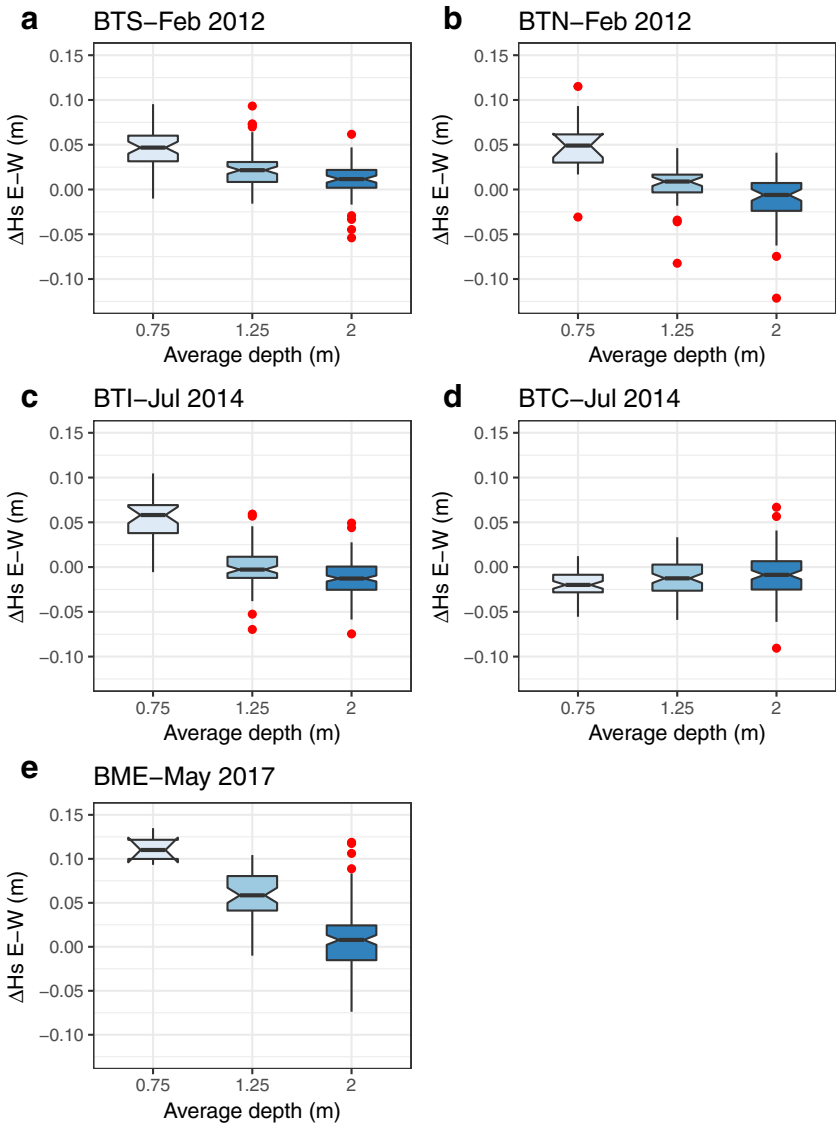

Fig. 9 Change in significant wave height as a function of water depth during wave events, defined as times when waves were greater than one standard deviation above the mean during each deployment. The event threshold wave height was 0.07 m in February 2012 (**a** BTS and **b** BTN); 0.13 m in July 2014 (**c** BTI and **d** BTC); and 00.17 m in May 2017 (**e** MBE). Notches in the box plots indicate confidence intervals around the mean. Boxes extend from the 25th to 75th percentiles, and the central lines show the 5th and 95th percentiles. The dots are conditions that fall outside this range

1.0 m, bracketing the elevations of the reef crests. This pattern of wave height change as a function of water depth was consistent for the four reefs, despite differences in the material comprising the reefs, their shape, reef orientation and proximity relative to the shoreline, wind conditions and whether all waves or just wave events were considered (Figs. 6 and 9). The elevations of the reef crests, 0.30–0.45 m below MSL, are below the growth ceiling for intertidal oyster reefs, observed to be on the order of 0.1 m below MSL for an estuary in North Carolina (Rodriguez et al. 2014). In fact, the BTI reef has recruited a significant oyster population since its installation in 2013–2014. As reefs grow vertically, the range of water depths associated with the greatest wave attenuation will shift upward. However, our results indicate that the greatest change in wave heights across a reef will still occur when water depths are within roughly ± 0.25 m of the elevation of the reef crest.

Within a ± 0.25-m range of water depths relative reef crest elevation, there are three possible relationships between the waves on one side of a reef and the other. For water depths on the low end of the range, the reef crest would be above the water surface for all but possibly the largest individual waves. In this case, any waves on the downwind side are likely to be the result of wave diffraction around the reef, locally generated waves, or waves propagating along the back side of the reef. Water depths in the middle of the range are comparable with the height of the reef crest. We therefore expect waves to be strongly modified or break as they cross the reef. When water depths are near the top of this range, the reef crest is submerged and waves may be able to propagate across the reef, with dissipation of wave energy owing to interactions of the oscillatory flow and the reef crest. As water depths continue to increase, the frictional interaction between the waves and reef crest diminishes, especially for the relatively narrow reefs in this study. Because the period of these waves was on the order of 2 s, their orbital

Table 5 Reductions in wave heights exceeding event threshold as a function of depth

Site	Depth range		
	0.5–1.0 m	1.0–1.5 m	1.5–2.5 m
BTS			
ΔHs (m)	0.046 ± 0.008	0.023 ± 0.005	0.010 ± 0.005
%ΔHs	48 ± 7	20 ± 4	8 ± 4
BTN			
ΔHs (m)	0.048 ± 0.021	0.006 ± 0.008	− 0.011 ± 0.008
%ΔHs	32 ± 13	20 ± 6	6 ± 4
BTI			
ΔHs (m)	0.053 ± 0.011	0.001 ± 0.005	− 0.012 ± 0.003
%ΔHs	35 ± 7	0 ± 3	− 6 ± 2
BTC			
ΔHs (m)	− 0.019 ± 0.005	− 0.014 ± 0.005	− 0.007 ± 0.005
%ΔHs	− 12 ± 3	− 7 ± 3	− 4 ± 3
MBE			
ΔHs (m)	0.096 ± 0.014	0.042 ± 0.009	0.009 ± 0.007
%ΔHs	47 ± 7	17 ± 3	3 ± 2

Event threshold is defined as one standard deviation above the mean significant wave height during each deployment period. For the February 2012 deployment, the threshold was 0.07 m; for the July 2014 deployment, the threshold was 0.13 m; for the May 2017 deployment, the threshold (at the inner site) was 0.17 m

motion at the level of the reef crest was significantly diminished by even 0.5 m of water over the reef.

To illustrate the relationship between waves on either side of the reefs, we examined several of the individual 5-min-long, 4-Hz wave time series, focusing on times when wind speeds were on the order of 6–8 m/s and water depths ranged from 0.6 to 1.3 m. Spectra during these times indicate only small changes in spectral form (Fig. 8) and average wave height (Table 4) when water depths are > 1.0 m (Dp-NE and Dp-SW). Spectra for water depths < 1.0 m (Sh and In cases in Fig. 8) were more variable, in some cases showing almost no waves on the sheltered side (e.g., BTS-199), in others a modified spectrum (e.g., BTS-589) and in still others, similar spectra on both sides of the reef (e.g., BTS-448) (Fig. 8; Table 4). Some of this variability may be due to the orientation of the BTS and BTI reef crests in the NNE-SSW directions, roughly paralleling the direction of the dominant winds, as noted above. In addition, because of the variability in wind directions and therefore the direction of wave propagation, the pair of wave gauges at each reef was seldom in line with the direction of wave motion. As a result, the downwind gauge was generally not recording the same specific set of waves as the upwind gauge. A more detailed investigation of wave transformation, including dissipation, refraction, and diffraction, by the reefs would require the use of a number of directional wave gauges spanning the reefs.

The reefs in our study were constructed for oyster habitat and, in some cases, shoreline protection. As a result, they are all located at least far enough offshore of the marsh shoreline for the reef crests to be below mean sea level, thereby allowing oyster recruitment over the reef surface. We did not consider any reefs constructed to be in contact with the marsh shoreline, such as a marsh toe revetment, although such reefs may also provide oyster habitat (Drexler et al. 2014; Theuerkauf et al. 2015). The reefs considered in our study are representative of many of the older and more recent constructed reefs in the Virginia coastal bays. Our sample size is small however, and similar or more detailed measurements over a wider range of reefs will be valuable for assessing the generality of our results.

Potential for Reef-Associated Wave Change to Benefit Adjacent Marshes

Our results indicate that the reefs we studied were most effective at attenuating wave energy when water depths were below mean sea level. When depths were very shallow (MLW-MLLW), waves were small no matter what (Fig. 7a). As depth increased, and with it the potential for larger waves, the reefs were able to reduce event wave heights (defined as wave heights greater than a standard deviation above the mean) by an average of 30–50% for water depths of 0.5–1.0 m (bracketing heights of reef crests) and 0–20% for water depths of 1.0–1.5 m (Table 5; Fig. 9). For water depths greater than 1.5 m, there was < 10% change in event wave heights across the four reefs.

Tonelli et al. (2010) concluded that the most effective waves for driving marsh-edge erosion are those that reach the marsh scarp when water levels are close to the elevation of the marsh platform. In general, the higher the marsh-edge scarp, the deeper the water is over the adjacent tidal flat when the water surface is at the elevation of the marsh platform. The deeper the water, the larger the waves for a given wind speed, and the greater the thrust the waves can impart to the marsh edge (Tonelli et al. 2010). When water depths are significantly higher than the elevation of the marsh platform, waves propagate across the marsh edge and dissipate their energy on the marsh platform rather than on the marsh edge.

Marsh platforms are most commonly found at elevations between MSL and MHHW (mean higher high water; Fagherazzi et al. 2013). Our results indicate that marshes with edge elevations close to mean sea level are most likely to benefit from reductions in wave energy associated with oyster reefs like those in our study area. For these marshes, the elevation of the marsh edge coincides with the water depths for which nearby oyster reefs have the greatest effect on wave height. As a result, the reefs have the potential to reduce the energy of the waves most likely to drive edge erosion, thereby helping to stabilize the location of the marsh edge. During

high tide and storm surge conditions, waves will propagate over the low-elevation marsh edge and dissipate within the marsh canopy due to interactions with marsh vegetation (Möller et al. 1999; Möller et al. 2014; Ferguson 2018), provided the marsh is sufficiently wide.

Low-elevation marsh edges are relatively common along the mainland marsh fringe of the Virginia coastal bays. For example, mainland marsh elevations in our study (BTS, BTN, and BTI) are mostly close to MSL in elevation, with little to no marsh-edge scarp (Fig. 10a, taken of the shoreline to the west of BTI) and shoreline erosion rates are generally low in the region to the west of the reefs, averaging -0.2 m year^{-1} $\pm$ 0.7 m (standard deviation), except locally near a channel mouth west of BTS (Fig. 1a). These rates are considerably smaller than rates at MBE (rates >1.0 m year^{-1}; Fig. 1b) and several other marsh island and backbarrier marsh sites (McLoughlin et al. 2015), largely owing to differences in fetch and wave exposure, but still reflect a general trend of shoreline erosion.

Marsh-edge elevations associated with marsh islands and backbarrier marshes in the Virginia coastal bays are commonly located higher in the tidal frame (between MSL and mean high water (MHW), which is about 0.6 m in the VCR), with a significant scarp on the order of 1 m high between the marsh platform and the adjacent tidal flat (Fig. 10b; McLoughlin et al. 2015) as is characteristic of many stable intertidal salt marshes (Morris et al. 2002; Fagherazzi et al. 2006). The scarp at our MBE site is quite small (~ 0.1 m), but portions of the Man and Boy shoreline have a much higher scarp. Our results indicate that oyster reefs are relatively ineffective at reducing wave energy when water depths are above MSL. This means that marsh edges characterized by relatively high vertical scarps with marsh surface elevations close to MHW will experience almost no decrease in wave energy due to fringing oyster reefs when water levels are close to the elevation of the marsh platform. As these are the wave and water-level conditions most effective at driving marsh-edge erosion, it is unlikely that fringing oyster reefs would significantly slow rates of retreat for these marshes.

Recent studies in the VCR and elsewhere have concluded that marsh-edge erosion rates have been relatively constant over the last 50 years (e.g., McLoughlin et al. 2015) and vary linearly in proportion to wave power at the marsh boundary (e.g., Marani et al. 2011; McLoughlin et al. 2015; Leonardi et al. 2016). Based on wave and marsh-edge erosion data from eight sites in the USA, Leonardi et al. (2016) determined that maximum marsh-edge erosion is associated with modestly-sized storms with a recurrence interval of 2.5 ± 0.5 month. This is in part because of their high frequency (Leonardi et al. 2016) but also because the storms that produce the largest waves are often accompanied by storm surge which allows much of the wave energy to pass across marsh boundaries. While oyster reefs with crests below MSL are unlikely to be effective at reducing the wave heights associated with high wind, storm surge conditions, our results support the conclusion that fringing oyster reefs are effective at reducing the wave energy reaching low-elevation marsh shorelines during the smaller, more-frequent storms that tend to drive marsh retreat.

Conclusions

Wave and water-level measurements collected across four restored oyster reefs in a system of shallow coastal bays show that they can be effective at reducing wave energy, but their effect is greatest when water depths are no more than a few tens of centimeters above the reef crest. Intertidal reef crest elevation is limited by aerial-exposure stress, resulting in a growth ceiling just below mean sea level (Rodriguez et al. 2014). As a consequence, intertidal fringing oyster reefs are most likely to be effective at attenuating moderately sized

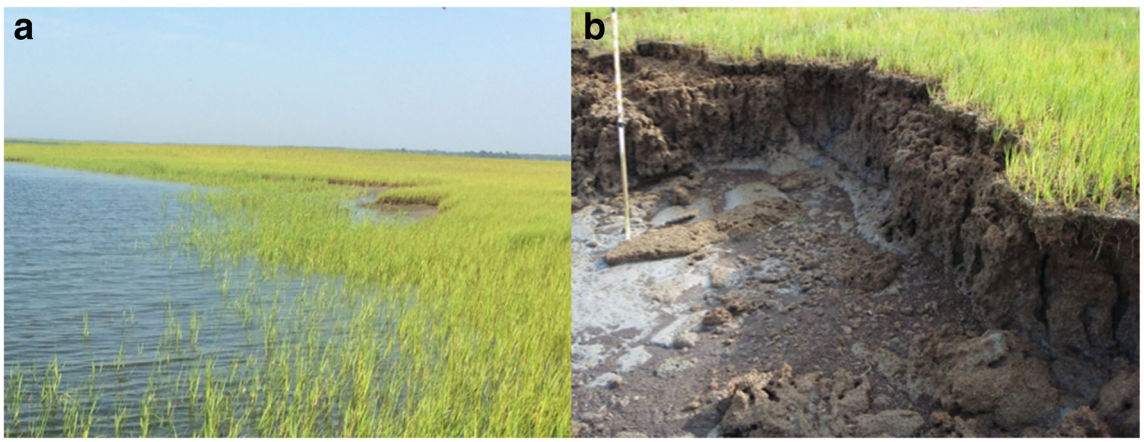

Fig. 10 Examples of **a** low elevation and **b** high elevation marsh edges. **a** A section of the marsh shoreline just west of Idaho Reef (site BTI; photo courtesy of Amy Ferguson). **b** A section of the marsh shoreline on Chimney Pole, a marsh island at the northern border of Hog Island Bay (McLoughlin et al. 2015)

wind-driven waves that are able to persist when water depths are near mean sea level or below. These waves are the primary driver of marsh-edge retreat for marshes with marsh-edge elevations that are close to mean sea level. In the Virginia coastal bays, low-lying marsh edges are most prevalent along the mainland margin of the bays, which is also the portion of marsh in the system most likely to be privately owned and targeted for shoreline protection. By attenuating wave energy at low- to mid-water levels, fringing reefs may help to stabilize low-elevation marsh edges. When water surface elevations are high, waves will propagate over low-elevation marsh edges and onto the marsh platform where marsh vegetation can provide effective wave attenuation. However, because reefs like those in our study have little effect on waves during deeper water conditions, which allow for the largest waves, they are less likely to offer protection to marshes characterized by high edge scarps and marsh surface elevations well above mean sea level.

Acknowledgements We thank the staff of the Anheuser-Busch Coastal Research Center and The Nature Conservancy for logistical support, particularly David Boyd (ABCRC) and Bo Lusk (TNC).

Funding Information This research was supported by the National Science Foundation through the VCR LTER award 1237733 and by a grant from the National Fish and Wildlife Foundation to The Nature Conservancy (2300.14.042551).

References

Coen, L.D., R.D. Brumbaught, D. Bushek, R. Grizzle, M.W. Luckenbach, M.H. Posey, S.P. Powers, and S.G. Tolley. 2007. Ecosystem services related to oyster restoration. *Marine Ecology Progress Series* 341: 303–307.

Dame, R.F., and B.C. Patten. 1981. Analysis of energy flows in an intertidal oyster reef. *Marine Ecology Progress Series* 5: 115–124.

Day, J.W., Jr., F. Scarton, A. Rismondo, and D. Are. 1998. Rapid deterioration of a salt marsh in Venice lagoon, Italy. *Journal of Coastal Research* 14: 583–590.

Drexler, M., M.L. Parker, S.P. Geiger, W.S. Arnold, and P. Hallock. 2014. Biological assessment of eastern oysters (*Crassostrea virginica*) inhabiting reef, mangrove, seawall, and restoration substrates. *Estuaries and Coasts* 37 (4): 962–972. https://doi.org/10.1007/s12237-013-9727-8.

Emery, K.A. 2015. Man and boy marsh shoreline change. Report for The Nature Conservancy.

Fagherazzi, S., L. Carniello, L. D'Alpaos, and A. Defiina. 2006. Critical bifurcation of shallow microtidal landforms in tidal flats and salt marshes. *Proceedings of the National Academy of Sciences* 103 (22): 8337–8341. https://doi.org/10.1073/pnas.0508379103.

Fagherazzi, S., G. Mariotti, J.H. Porter, K.J. McGlathery, and P.L. Wiberg. 2010. Wave energy asymmetry in shallow bays. *Geophysical Research Letters* 72 (24): L24601. https://doi.org/10.1029/2010GL045254.

Fagherazzi, S., P.L. Wiberg, S. Temmerman, E. Struyf, Y. Zhao, and P.A. Raymond. 2013. Fluxes of water, sediment, and biogeochemical compounds in salt marshes. *Ecological Processes* 2 (1): 3.

Ferguson, A.E. 2018. Evaluating nature-based solutions to storm wave impacts in the Virginia coast reserve. M.S. Thesis, University of Virginia, Charlottesville, VA, 188 pp.

Huang, Z.-C., L. Lenain, W.K. Melville, J.H. Middleton, B. Reineman, N. Statom, and R.M. McCabe. 2012. Dissipation of wave energy and turbulence in a shallow coral reef lagoon. *Journal of Geophysical Research* 117: C03015. https://doi.org/10.1029/2011JC007202.

Jackson, C.W., C.R. Alexander, and D.M. Bush. 2012. Application of the AMBUR R package for spatio-temporal analysis of shoreline change: Jekyll Island, Georgia, USA. *Computers & Geosciences* 41: 199–207. https://doi.org/10.1016/j.cageo.2011.08.009.

Kathilankal, J.C., T.J. Mozdzer, J.D. Fuentes, P. D'Odorico, K.J. McGlathery, and J.C. Zieman. 2008. Tidal influences on carbon assimilation by a salt marsh. *Environmental Research Letters* 3 (4): 044010. https://doi.org/10.1088/1748-9326/3/4/044010.

Leonardi, N., N.K. Ganju, and S. Fagherazzi. 2016. A linear relationship between wave power and erosion determines salt-marsh resilience to violent storms and hurricanes. *Proceedings of the National Academy of Sciences* 113 (1): 64–68. https://doi.org/10.1073/pnas.1510095112.

Lowe, R.J., J.L. Falter, M.D. Bandet, G. Pawlak, M.J. Atkinson, S.G. Monismith, and J.R. Koseff. 2005. Spectral wave dissipation over a barrier reef. *Journal of Geophysical Research* 110: C04001. https://doi.org/10.1029/2004JC002711.

Malhotra, A., and M.S. Fonseca. 2007. WEMo (Wave Exposure Model): Formulation, Procedures and Validation.NOAA Technical Memorandum NOS NCCOS 65. NOAA/National Ocean Service/National Centers for Coastal Ocean Science, Beaufort, NC, 28 pp.

McLoughlin, S.M., P.L. Wiberg, I. Safak, and K.J. McGlathery. 2015. Rates and forcing of marsh edge erosion in a shallow coastal bay. *Estuaries and Coasts* 38 (2): 620–638. https://doi.org/10.1007/s12237-014-9841-2.

Marani, M., A. D'Alpaos, S. Lanzoni, and M. Santalucia. 2011. Understanding and predicting wave erosion of marsh edges. *Geophysical Research Letters* 38 (21): L21401. https://doi.org/10.1029/2011GL048995.

Mariotti, G., and S. Fagherazzi. 2013. Critical width of tidal flats triggers marsh collapse in the absence of sea-level rise. *Proceedings of the National Academy of Sciences* 110 (14): 5353–5356. https://doi.org/10.1073/pnas.1219600110.

Meyer, D.L., E.C. Townsend, and G.W. Thayer. 1997. Stabilization and erosion control value of oyster cultch for intertidal marsh. *Restoration Ecology* 5 (1): 93–99.

Möller, I., T. Spencer, J.R. French, D.J. Leggett, and M. Dixon. 1999. Wave transformation over salt marshes: a field and numerical modeling study from North Norfolk, England. *Estuarine Coastal and Shelf Science* 49 (3): 411–426.

Möller, I., M. Kudella, F. Rupprecht, T. Spencer, M. Paul, B.K. van Wesenbeeck, G. Wolters, K. Jensen, T.J. Bouma, M. Miranda-Lange, and S. Schimmels. 2014. Wave attenuation over coastal salt marshes under storm surge conditions. *Nature Geoscience* 7 (10): 727–731. https://doi.org/10.1038/ngeo2251.

Morris, J.T., P.V. Sundareshwar, C.T. Nietch, B. Kjerfve, and D.R. Cahoon. 2002. Responses of coastal wetlands to rising sea level. *Ecology* 83 (10): 2869–2877.

Piazza, B.P., P.D. Banks, and M.K. La Peyre. 2005. The potential for created oyster shell reefs as a sustainable shoreline protection strategy in Louisiana. *Restoration Ecology* 13 (3): 499–506.

Rodriguez, A.B., F.J. Fodrie, J.T. Ridge, N.L. Lindquist, E.J. Theuerkauf, S.E. Coleman, J.H. Grabowski, M.C. Brodeur, R.K. Gittman, D.A. Keller, and M.D. Kenworthy. 2014. Oyster reefs can outpace sea-level rise. *Nature Climate Change* 4 (6): 493–497. https://doi.org/10.1038/nclimate2216.

Safak, I., P.L. Wiberg, M.O. Kurum, and D.L. Richardson. 2015. Controls on residence time and exchange in a system of shallow coastal bays. *Continental Shelf Research* 97: 7–20. https://doi.org/10.1016/j.csr.2015.01.009.

Schwimmer, R.A. 2001. Rates and processes of marsh shoreline erosion in Rehoboth Bay, Delaware, U.S.A. *Journal of Coastal Research* 17: 672–683.

Scyphers, S.B., S.P. Powers, K.L. Heck Jr., and D. Byron. 2011. Oyster reefs as natural breakwaters mitigate shoreline loss and facilitate fisheries. *PLoS One* 6 (8): e22396. https://doi.org/10.1371/journal.pone.0022396.

Stricklin, A.G., M.S. Peterson, J.D. Lopez, C.A. May, C.F. Mohrann, and M.S. Woodrey. 2009. Do small, patchy, constructed intertidal oyster reefs reduce salt marsh erosion as well as natural reefs? *Gulf and Caribbean Research* 22: 21–27.

Taube, S.R. 2013. Impacts of fringing oyster reefs on wave attenuation and marsh erosion rates. M.S. thesis, University of Virginia, Charlottesville, VA, 157pp.

Theuerkauf, S.J., R.P. Burke, and R.N. Lipcius. 2015. Settlement, growth, and survival of eastern oysters on alternative reef substrates. *Journal of Shellfish Research* 34: 241–250. https://doi.org/10.2983/035.034.0205.

Tonelli, M., S. Fagherazzi, and M. Petti. 2010. Modeling wave impact on salt marsh boundaries. *Journal of Geophysical Research* 115: C09028. https://doi.org/10.1029/2009JC006026.

van der Wal, D., and K. Pye. 2004. Patterns, rates and possible causes of saltmarsh erosion in the Greater Thames area (UK). *Geomorphology* 61: 373–391.

Whitman, E.R., and M.A. Reidenbach. 2012. Benthic flow environments affect recruitment of *Crassostrea virginica* larvae to an intertidal oyster reef. *Marine Ecology Progress Series* 463: 117–191.

Wiberg, P.L., and C.R. Sherwood. 2008. Calculating wave-generated bottom orbital velocities from surface-wave parameters. *Computers & Geosciences* 34 (10): 1243–1262.

Wilson, C.A., and M.A. Allison. 2008. An equilibrium profile model for retreating marsh shorelines in Southeast Louisiana. *Estuarine Coastal and Shelf Science* 80 (4): 483–494.

Woodhouse, W.E., Jr., and P.L. Knutson. 1982. Atlantic coastal marshes. In *Creation and restoration of coastal plant communities*, ed. R.R. Lewis III. Boca Raton: CRC Press, Inc. 219 p.

Wray, R.D., S.P. Leatherman, and R.J. Nicholls. 1995. Historic and future land loss for upland and marsh islands in the Chesapeake Bay, Maryland, U.S.A. *Journal of Coastal Research* 11: 1195–1203.

Wunsch, C., and D. Stammer. 1997. Atmospheric loading and the oceanic "inverted barometer" effect. *Reviews of Geophysics* 35 (1): 79–107.